

Temperature Regulation of Crown-Mediated Ion Transport through Polymer/Liquid Crystal Composite Membranes. Remarkable Transport Ability of Fluorocarbon-Containing Crown Ethers

Seiji Shinkai,*¹ Kazufumi Torigoe,¹ Osamu Manabe,¹ and Tisato Kajiyama²

Contribution from the Department of Industrial Chemistry, Faculty of Engineering, Nagasaki University, Nagasaki 852, Japan, and the Department of Applied Chemistry, Faculty of Engineering, Kyushu University, Fukuoka 812, Japan. Received January 2, 1987

Abstract: Ternary composite membranes composed of polymer (polycarbonate, PC), liquid crystal [*N*-(4-ethoxybenzylidene)-4'-butylaniline, EBBA], and crown ethers having a hydrocarbon chain (**1a**, **1b**, and **1c**) or a fluorocarbon chain (**2b** and **2c**) have been prepared. The DSC study established that the hydrocarbon-containing crown ethers are dissolved homogeneously in the PC/EBBA membrane, whereas the fluorocarbon-containing crown ethers form microheterogeneous, phase-separated aggregates in the membrane. Transport of K⁺ ion through the PC/EBBA/**1** membranes occurred below and above T_{KN} (crystal-nematic liquid crystal phase-transition temperature of EBBA, 305 K), and the transport rates were faster above T_{KN} . This indicates that carrier-mediated K⁺ transport is directly affected by the fluidity of the membrane phase. The PC/EBBA/**2** membranes provided two unexpected transport characteristics: (i) K⁺ transport through these membranes is "completely" suppressed below T_{KN} and (ii) K⁺ was transported rapidly above T_{KN} (21–23 times faster than with the PC/EBBA/**1a** membrane). This unusual transport ability was rationalized, on the basis of the DSC studies and the thermodynamic studies, in terms of "phase-separation" and "desolvation" characteristic of the fluorocarbon-containing crown ethers. The Arrhenius thermodynamic parameters showed a good enthalpy–entropy compensation relationship ($r = 0.999$) expressed by $\log E_a$ (kJ mol⁻¹) = 5.69 log A + 52.7, but the transport rates were correlated with the increase in the entropy term. This supports the importance of the membrane fluidity in efficient ion transport. The PC/EBBA/**2b** membrane was applied to ion-selective membrane transport and to temperature regulation of ion transport rates. The membrane transport data showed a pronounced K⁺ selectively probably because of the formation of a 1:2 metal–crown sandwich complex between K⁺ and aggregated **2b**. Also, we could observe a reversible, all-or-nothing change in the K⁺ transport rate that was induced by the on–off-type temperature change. Thus, the PC/EBBA/**2** membranes act as an ideal thermocontrolled system for K⁺ transport: no transport below T_{KN} and very efficient transport above T_{KN} .

In the past, two different types of membranes have been used in membrane transport systems: liquid membranes and polymeric membranes.³ Each type of membrane has advantages and disadvantages. A liquid membrane is very convenient and can provide a large transport flux, but the system is not necessarily useful for practical applications. On the other hand, a polymeric membrane is more useful for practical applications but is often hampered by a low transport flux. If one could develop a new membrane which would compensate for these disadvantages, it would be very useful not only for laboratory-scale transport experiments but also for practical membrane separations. The polymer/liquid crystal composite membrane, in which the liquid crystalline material is embedded in a polymer matrix, can satisfy these requirements. It is apparently a polymeric solid membrane but can provide a relatively large transport flux above the crystal–liquid crystal phase-transition temperature (T_{KN}).^{4–8} This is due to the high fluidity of the liquid crystalline material which forms the continuous phase in the polymer matrix.^{4–8} It could be called "a liquid membrane in polymer clothing" or "an immobilized liquid membrane". Another interesting feature of the polymer/liquid

crystal composite membrane is related to thermocontrol of permeation rates. Thermal molecular motion of the liquid crystalline material changes drastically at T_{KN} , so that the permeation efficiency across this membrane changes discontinuously at this temperature. It is known that a distinct increase in the thermal molecular motion at T_{KN} causes a rapid increase in water or gas permeability coefficients.^{4,5,8} One may consider, therefore, that polymer/liquid crystal composite membranes possess biomembrane-mimetic properties with respect to the phase-transition phenomena.^{9–22}

We now report the temperature regulation of carrier-mediated ion transport through ternary composite membranes composed

(1) Nagasaki University.

(2) Kyushu University.

(3) Kesting, R. E. In *Synthetic Polymeric Membranes*; Wiley: New York, 1985.

(4) Kajiyama, T.; Nagata, Y.; Washizu, S.; Takayanagi, M. *J. Membr. Sci.* **1982**, *11*, 39.

(5) Washizu, S.; Terada, I.; Kajiyama, T.; Takayanagi, M. *Polym. J. (Tokyo)* **1984**, *16*, 307.

(6) (a) Shinkai, S.; Nakamura, S.; Tachiki, S.; Manabe, O.; Kajiyama, T. *J. Am. Chem. Soc.* **1985**, *107*, 3363. (b) Shinkai, S.; Nakamura, S.; Ohara, K.; Tachiki, S.; Manabe, O.; Kajiyama, T. *Macromolecules* **1987**, *20*, 21.

(7) Shinkai, S.; Torigoe, K.; Manabe, O.; Kajiyama, T. *J. Chem. Soc., Chem. Commun.* **1986**, 933.

(8) For a comprehensive review on polymer/liquid crystal composite membranes, see: Kajiyama, T.; Washizu, S.; Kumano, A.; Terada, I.; Takayanagi, M.; Shinkai, S. *J. Appl. Polym. Sci., Appl. Polym. Symp.* **1985**, *41*, 327.

(9) (a) Kunitake, T. *J. Macromol. Sci. Chem.* **1979**, *A13*, 586. (b) Kunitake, T. *Makromol. Chem.* **1979**, *4*, 166.

(10) (a) Fendler, J. H. *Acc. Chem. Res.* **1980**, *13*, 7. (b) Fendler, J. H. In *Membrane Mimetic Chemistry*; Wiley: New York, 1982.

(11) Kajiyama, T.; Kumano, A.; Takayanagi, M.; Okahata, Y.; Kunitake, T. *Chem. Lett.* **1979**, 645.

(12) Tundo, P.; Kippenberger, D. J.; Klahn, P. L.; Prieto, N. E.; Jao, T.-C.; Fendler, J. H. *J. Am. Chem. Soc.* **1982**, *104*, 456.

(13) Kippenberger, D. J.; Rosenquist, K.; Odberg, L.; Tundo, P.; Fendler, J. H. *J. Am. Chem. Soc.* **1983**, *105*, 1129.

(14) Reed, W.; Guterman, L.; Tundo, P.; Fendler, J. H. *J. Am. Chem. Soc.* **1984**, *106*, 1897.

(15) Regen, S. L.; Czech, B.; Singh, A. *J. Am. Chem. Soc.* **1980**, *102*, 6638.

(16) Regen, S. L.; Singh, A.; Oehme, G.; Singh, M. *J. Am. Chem. Soc.* **1982**, *104*, 791.

(17) Regen, S. L.; Shin, J.-S.; Yamaguchi, K. *J. Am. Chem. Soc.* **1984**, *106*, 2446.

(18) Johnston, D. S.; Sanghera, S.; Pons, M.; Chapman, D. *Biochim. Biophys. Acta* **1980**, *602*, 57.

(19) Lopez, E.; O'Brien, D. F.; Whitesides, T. H. *J. Am. Chem. Soc.* **1982**, *104*, 305.

(20) Gros, L.; Ringsdorf, H.; Schupp, H. *Angew. Chem., Int. Ed. Engl.* **1981**, *20*, 305.

(21) Roks, M. F. M.; Visser, H. G. J. *Zwicker, J. W.; Verkley, A. J.; Nolte, R. J. M. J. Am. Chem. Soc.* **1983**, *105*, 507.

(22) Kunitake, T.; Nakashima, N.; Takarabe, N.; Nagai, M.; Tsuge, A.; Yanagi, H. *J. Am. Chem. Soc.* **1981**, *103*, 5945.

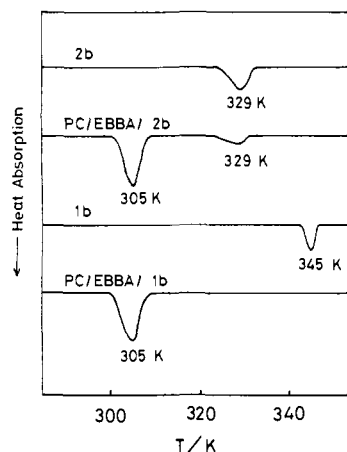
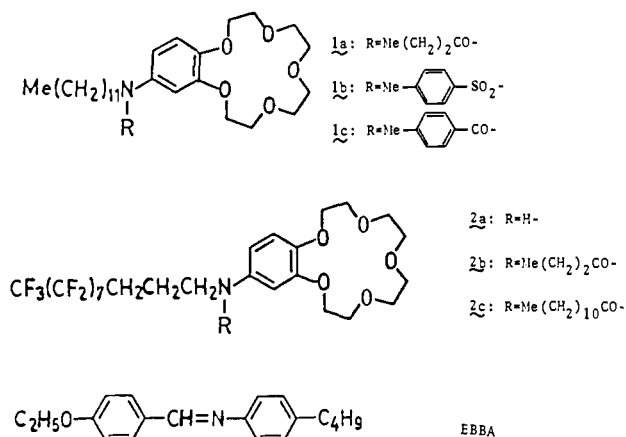


Figure 1. DSC curves for carriers **1b** and **2b** and their composite membranes.

of polymer (polycarbonate, PC), liquid crystal [*N*-(4-ethoxybenzylidene)-4'-butylaniline, EBBA], and hydrocarbon- (**1a**, **1b**, and **1c**) or fluorocarbon-containing crown ethers (**2a**, **2b**, and **2c**).



We have found that the rate of ion transport is profoundly related to the fluidity of the EBBA phase and also to the phase separation of the crown ether in the composite membrane. In particular, when the fluorocarbon-containing crown ethers which form microheterogeneous, phase-separated aggregates in the membrane phase were used as ion carriers, ion transport below T_{KN} was suppressed "completely" while large ion fluxes were found above T_{KN} , resulting in a dramatic rate change at T_{KN} . This is a novel method for the efficient temperature regulation of ion transport with a polymer/liquid crystal composite membrane system.

Results and Discussion

Dispersion State of Crown Ethers in the Composite Membrane.

The composite membrane is a blend film prepared by casting a 1,2-dichloroethane solution of PC (40 wt %) and EBBA (60 wt %). It has been established that in the composite membrane EBBA forms a continuous phase across the polymer matrix and exhibits a crystal-nematic liquid crystal phase transition at 304–305 K.⁸ One of the main objectives of this investigation is to clarify a potential relation between the ion transport ability and the dispersion state of the carriers in a composite membrane. In order to change the "solubility" of crown ethers in the membrane, we synthesized hydrocarbon-containing **1** and fluorocarbon-containing **2**. When 1,2-dichloroethane solutions of **1** (4.3 mol % of EBBA), PC, and EBBA were cast on a glass plate, transparent homogeneous membranes suitable for membrane transport experiments were obtained. In contrast, **2a** (4.3 mol % of EBBA) gave a phase-separated white layer above the PC/EBBA layer. This suggests that **2a** is immiscible with the PC/EBBA membrane because of the lipophobic nature of the fluorocarbon chain. To enhance the miscibility, we synthesized **2b** and **2c**, which possess an additional hydrocarbon chain. As

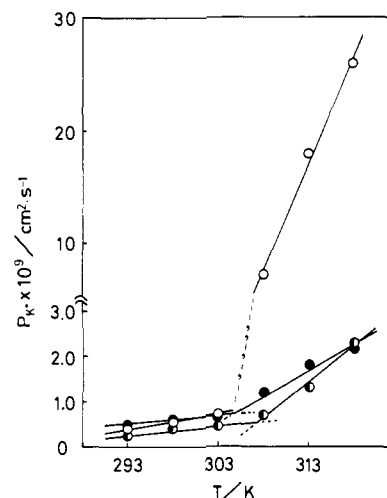


Figure 2. Temperature dependence of P_{K^+} for the composite membranes of hydrocarbon-containing crown ethers: PC/EBBA/**1a** (●), PC/EBBA/**1b** (○), and PC/EBBA/**1c** (○).

expected, **2b** and **2c** gave "apparently" homogeneous membranes when cast from 1,2-dichloroethane solutions.

The dispersion state of the crown ethers in the PC/EBBA/crown ternary composite membrane was studied by DSC (Figure 1). The PC/EBBA binary composite membrane gave an endothermic peak at 305 K, which corresponds to the crystal-nematic liquid crystal phase-transition temperature (T_{KN}) of the EBBA phase. The PC/EBBA/**2b** membrane gave two endothermic peaks at 305 and 329 K that are assigned to the T_{KN} of EBBA and the melting point of **2b**, respectively. Thus, **2b** is shown to form microheterogeneous, phase-separated aggregates in the composite membrane. The phase separation is caused by the poor miscibility of the fluorocarbon chain with the hydrocarbonic membrane phase. On the other hand, the PC/EBBA/**1b** membrane (mp of **1b**, 344–346 K) gave only one peak at 305 K and did not show any perceptible absorption peak at 344–346 K, the melting point of **1b**. Therefore, **1b** should dissolve homogeneously in the composite membrane. Unfortunately, **1a**, **1c**, and **2c** were isolated as oily compounds, so their dispersion states could not be established by the DSC method. On the basis of the structural similarity, it is expected that **1a** and **1c** containing a hydrocarbon substituent like **1b** would disperse homogeneously while **2c** containing a fluorocarbon chain like **2b** would form phase-separated aggregates in the composite membrane.

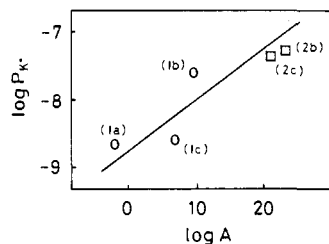
Temperature Regulation of K^+ Transport Rates. Since leaching of crown ethers into the aqueous phase from crown-containing polymeric membranes may be a serious complication,²³ it was important to demonstrate that our composite membranes were stable. Chipped pieces of the composite membrane were stirred in an aqueous solution at 30 °C for 24 h. HPLC analysis of the aqueous solutions demonstrated that five crown ethers are not leached (less than 1%) into the aqueous phases. Therefore, the crown ethers are shown to partition predominantly in the membrane phase, and the ternary composite membranes can be used safely for the ion transport experiments.

Transport experiments were conducted in a U-tube immersed in a thermostated water bath (for details see the Experimental Section). The source aqueous phase (IN phase) contained 0.30 M potassium *p*-toluenesulfonate, and the concentration of transported K^+ in the receiving aqueous phase (OUT phase) was measured as a function of time by atomic absorption spectroscopy. Figure 2 shows plots of the permeability coefficients for K^+ (P_{K^+}) vs. transport temperature for the PC/EBBA/**1** membranes. Transport of K^+ across the PC/EBBA/**1** membranes was observed below and above T_{KN} and was faster above T_{KN} , resulting in a clear break point near T_{KN} . Thus, carrier-mediated K^+ transport is directly affected by the molecular motion of EBBA and becomes

(23) Reinhoudt, D. N., private communication.

Table I. Permeability Coefficients (P_{K^+}) and Arrhenius Thermodynamic Parameters (E_a and $\log A$) for K^+ Transport

membrane	$10^9 P_{K^+}$ ($\text{cm}^2 \text{s}^{-1}$)		E_a (kJ mol $^{-1}$)		$\log A$	
	298 K	318 K	below T_{KN}	above T_{KN}	below T_{KN}	above T_{KN}
	PC/EBBA/1a	0.616	2.12	34.4	42.2	-3.16
PC/EBBA/1b	0.564	26.0	45.1	105	-1.39	9.72
PC/EBBA/1c	0.464	2.30	45.6	97.4	-1.38	7.38
PC/EBBA/2b	0	49.7		186		23.4
PC/EBBA/2c	0	44.6		172		20.9

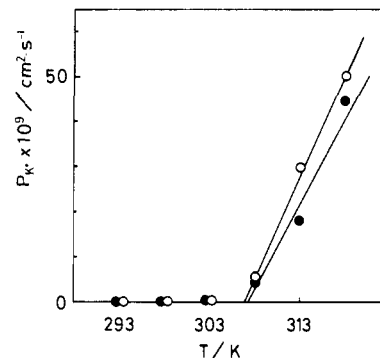
**Figure 3.** Correlation between $\log P_{K^+}$ and $\log A$ at 318 K.

more advantageous in the fluid liquid crystal phase. The PC/EBBA/1b membrane gave the largest P_{K^+} above T_{KN} . Arrhenius plots (not shown here) consisted of two straight lines intersecting at T_{KN} . The thermodynamic parameters (E_a and $\log A$) and typical P_{K^+} values are summarized in Table I.

The E_a values obtained for the PC/EBBA/1 membranes below T_{KN} (34.4–45.6 kJ mol $^{-1}$) are quite comparable with those for ion permeation across crown-immobilized polymeric membranes (ca. 50 kJ mol $^{-1}$).²⁴ It is known that, in the crown-immobilized polymeric membranes, ions are transported according to a "site-to-site jump" mechanism because the crown ethers themselves cannot diffuse across the membranes.²⁴ The similarity of the activation energies suggests that a similar jump mechanism is also operative in the crystalline PC/EBBA/1 membranes below T_{KN} . Therefore, the crown carriers do not diffuse through the crystal lattice of EBBA. On the other hand, the E_a values obtained for the PC/EBBA/1 membranes above T_{KN} (42.2–105 kJ mol $^{-1}$) are mostly greater than those for ion permeation across crown-immobilized polymeric membranes (ca. 50 kJ mol $^{-1}$)²⁴ but are a little smaller than those for carrier-mediated ion transport across liposomal membranes (90–130 kJ mol $^{-1}$).^{25–28} It is known that a carrier transport mechanism is mainly operative in the fluid liposomal membrane systems.^{25–28} The intermediate E_a values obtained for the PC/EBBA/1 membranes above T_{KN} suggest that K^+ is transported by both mechanisms, the jump mechanism and the carrier mechanism. This problem will be discussed later in more detail.

Table I also shows that the liquid crystal phase (above T_{KN}) gives E_a and $\log A$ values which are greater than those for the crystal phase (below T_{KN}). As shown in Figure 2, ion transport rates are considerably enhanced above T_{KN} . This result implies that P_{K^+} increases because of a favorable enhancement in $\log A$ in spite of the unfavorable E_a increase. In fact, P_{K^+} is correlated (although approximately) with the increase in the $\log A$ term (Figure 3) and almost inversely with the increase in the $-E_a/RT$ term. The observation that the transport rate is governed by the entropy term suggests that diffusion of the crown-metal complexes is a main rate-limiting step in the present transport system. In contrast, association-dissociation of the complexes which should be reflected in the enthalpy term would be less important.

The DSC studies established that the fluoro-containing crown ethers **2** form phase-separated aggregates in the composite membrane. What kind of the transport properties is expected for

**Figure 4.** Temperature dependence of P_{K^+} for the composite membranes of fluorocarbon-containing crown ethers: PC/EBBA/2b (O), PC/EBBA/2c (●).

such microheterogeneous membranes? The PC/EBBA/2 membranes provide two novel transport properties (Figure 4). First, K^+ transport through these membranes is "completely" suppressed below T_{KN} and increases with increasing transport temperature above T_{KN} . This unexpected finding indicates that ion transport through the crystal phase is profoundly influenced by the dispersion state of ion carriers and that the ion flux can be stopped completely by forming microheterogeneous carrier domains. Secondly, the fluorocarbon-containing **2** transports K^+ much faster than the hydrocarbon-containing **1** above T_{KN} (Table I). At 318 K, for example, the P_{K^+} values for **2b** and **2c** are greater by factors of 23.4 and 21.0, respectively, than that for **1a**. Comparison of the thermodynamic parameters indicates that above T_{KN} the $\log A$ values for **2b** and **2c** are markedly increased (by 25.1 and 22.6, respectively, compared with that of **1a**), but at the same time the E_a values increase 4.1–4.4-fold. As shown in Figure 3, however, the transport rate is actually governed by the $\log A$ term but not by the E_a term. Therefore, the remarkable enhancement of the P_{K^+} values of **2b** and **2c** must result from the "favorable entropy term".

What does favorable entropy term mean? It is well-known that fluorocarbon compounds generally exhibit lipophobic behaviors as well as the hydrophobic properties. In fact, **2a** is not miscible with the hydrocarbonic membrane phase. This suggests that **2b** and **2c**, which are barely dispersed in the membrane, are not "wet" by the EBBA molecules and are relatively "desolvated". Furthermore, they may disorder the liquid crystal structure of EBBA because of the aggregate formation. These situations would allow the rapid diffusion of the fluorocarbon-containing crown ethers through the membrane phase. This effect would be reflected in the entropy term. In any event, an ideal temperature-regulation system for K^+ transport is now realized: no transport below T_{KN} and very efficient transport above T_{KN} .

Why Was K^+ Transport Stopped Completely below T_{KN} ? Comments on the Transport Mechanism. It was very interesting to consider why K^+ transport was suppressed completely below T_{KN} in the PC/EBBA/2 membranes. Above T_{KN} the continuous EBBA phase is fluid, so that crown ethers can diffuse in the membrane phase as those in a liquid membrane system.^{29–32} This is the so-called carrier mechanism. Below T_{KN} , on the other hand, the carrier mechanism is no longer operative because crown ethers are fixed in the frozen, crystalline lattice of EBBA and cannot diffuse in the membrane. However, Figure 2 shows how K^+ transport still can take place across such a frozen membrane below T_{KN} when the crown ethers are homogeneously dispersed. In this case, ions are transported according to a site-to-site jump mechanism (Figure 5A) which generally proposed for crown-immobilized polymeric membranes.²⁴ When the carrier sites are dis-

(24) Shchori, E.; Jagur-Grodzinski, J. *J. Appl. Polym. Sci.* **1976**, *20*, 773.(25) Donis, J.; Grandjean, J.; Grosjean, A.; Laslo, P. *Biochem. Biophys. Res. Commun.* **1981**, *102*, 690 and references cited therein.(26) Degani, H. *Biochim. Biophys. Acta* **1978**, *509*, 364.(27) Hunt, G. R. A.; Tipping, L. R. H.; Belmont, M. R. *Biophys. Chem.* **1978**, *8*, 341.(28) Degani, H.; Lenkinski, R. E. *Biochemistry* **1980**, *19*, 3430.(29) Reusch, C. F.; Cussler, E. L. *AIChE J.* **1973**, *19*, 736.(30) (a) Fyles, T. M. *J. Membr. Sci.* **1985**, *24*, 229. (b) Fyles, T. M. *J. Chem. Soc., Faraday Trans. 1* **1986**, *82*, 617.(31) Strzelbicki, J.; Bartsch, R. A. *J. Membr. Sci.* **1982**, *10*, 35.(32) Lamb, J. D.; Christensen, J. J.; Oscarson, J. L.; Nielsen, B. L.; Asay, B. W.; Izatto, R. M. *J. Am. Chem. Soc.* **1980**, *102*, 6820.

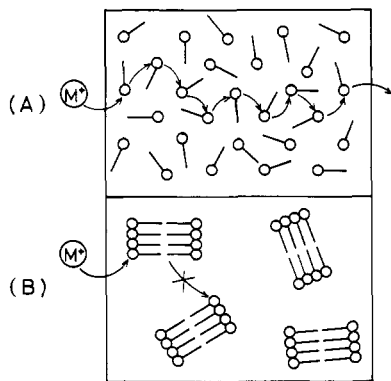


Figure 5. Schematic representation of the ion transport mechanisms below T_{KN} : (A) site-to-site jump mechanism for homogeneously dispersed membranes, (B) aggregate-to-aggregate (interaggregate) jump mechanism for microheterogeneous, phase-separated membranes.

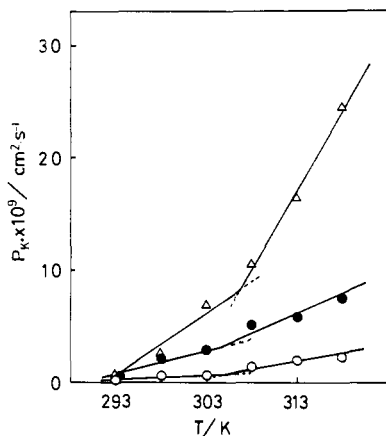


Figure 6. Influence of carrier **1a** concentration on P_{K^+} . The ratio of PC:EBBA was constant (40:60 wt/wt), and the **1a** concentration was varied: (O) 4.3 mol % of EBBA, (●) 6.4 mol % of EBBA, and (Δ) 8.6 mol % of EBBA.

persed homogeneously in the membrane (i.e., with PC/EBBA/1), the jump mechanism can easily occur because a metal cation complexed by a crown can easily find an adjacent crown for the jump. In contrast, when the carriers form the phase-separated aggregates in the membrane (i.e., with PC/EBBA/2), the distance is too far to jump, and an aggregate-to-aggregate (interaggregate) jump becomes almost impossible (Figure 5B). This would result in the complete suppression of ion transport below T_{KN} .

In order to test this hypothesis, the effect of the carrier concentration on the transport rates was examined. Figures 6 and 7 show the dependence of the K^+ transport rate on the carrier concentration. In the PC/EBBA/1a membrane, K^+ transport was observed below and above T_{KN} , and in every case a break point appeared near T_{KN} . Therefore, the jump mechanism should be consistently operative in the homogeneous 1a-containing membrane below T_{KN} . In the PC/EBBA/2b membrane an all-or-nothing change in P_{K^+} was observed when the 2b concentration was lower than 4.3 mol %, indicating that the interaggregate jump is inhibited below T_{KN} . Interestingly, when the 2b concentration was increased to 8.6 mol %, K^+ transport below T_{KN} was detectable for the first time. This finding suggests that there is a critical distance for the jump of K^+ in the crystalline EBBA phase. In other words, K^+ transport can be stopped completely when the distance between the aggregates is more than a critical distance. If the aggregation number of 2b in each aggregate can be determined, one could compute the critical distance for the K^+ jump. Several methods such as electron microscopy and molecular weight determination, etc. were attempted but failed.

In Figure 8, $\log P_{K^+}$ above T_{KN} is plotted against $\log [1a \text{ or } 2b]$. The slopes correspond to the dependence of the transport rate on the carrier concentration, which may be called the "transport order" similar to a "reaction order". Least-squares

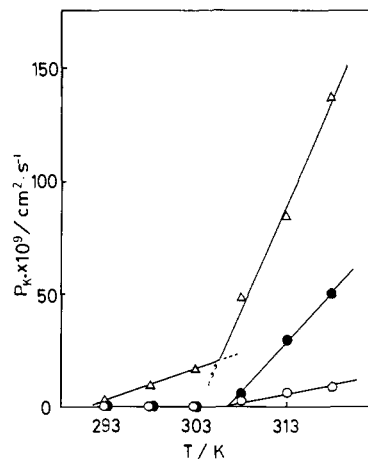


Figure 7. Influence of carrier **2b** concentration on P_{K^+} . The ratio of PC:EBBA was constant (40:60 wt/wt), and the **2b** concentration was varied: (O) 2.1 mol % of EBBA, (●) 4.3 mol % of EBBA, and (Δ) 8.6 mol % of EBBA.

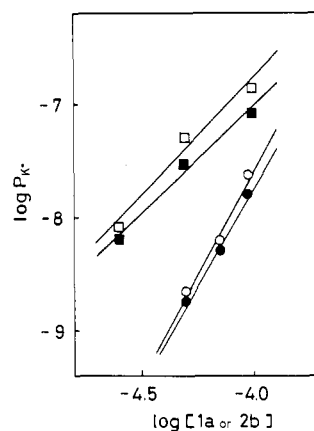


Figure 8. Plots of $\log P_{K^+}$ vs. logarithm of the carrier concentration (in mol % of EBBA): PC/EBBA/1a (●) at 313 K and (O) at 318 K; PC/EBBA/2b (■) at 313 K and (□) at 318 K.

computation gave the following slope values: for PC/EBBA/1a, slope = 3.4 at 313 K and 3.7 at 318 K; for PC/EBBA/2b, slope = 1.9 at 313 K and 2.1 at 318 K. In carrier-mediated ion transport across a liquid membrane, the transport rate is usually proportional to the first power of the carrier concentration.^{29,30,33} Therefore, the present system is not consistent with the simple carrier-mediated transport mechanism. On the other hand, the transport order for the site-to-site jump mechanism is not established clearly. This is due to a difficulty to accurately define the carrier concentration in the crown-immobilized polymeric membrane. The jump step can be regarded as an interaction between a metal-crown complex and an uncomplexed crown. Therefore, the transport rate ($\propto [\text{metal-crown}] \cdot [\text{uncomplexed crown}]$) should exhibit at least a second-order dependence on the carrier concentration. The transport orders (1.9–3.7) obtained for the PC/EBBA composite membranes suggest that even in the liquid crystal phase (above T_{KN}) not only the simple carrier mechanism but also the jump mechanism is operative. This is consistent with the fact that the PC/EBBA/1 membranes give intermediate E_a values between those for the carrier mechanism and the jump mechanism (vide ante).

Figure 9 shows a plot of $\log A$ vs. E_a for the PC/EBBA/1 membranes. Five points above T_{KN} give an excellent linear relationship ($r = 0.999$) expressed by eq 1. This indicates that the

$$E_a \text{ (kJ mol}^{-1}\text{)} = 5.71 \log A + 52.4 \quad (1)$$

change in the entropy term is compensated in part by the change in the enthalpy term even though P_{K^+} is actually governed by the

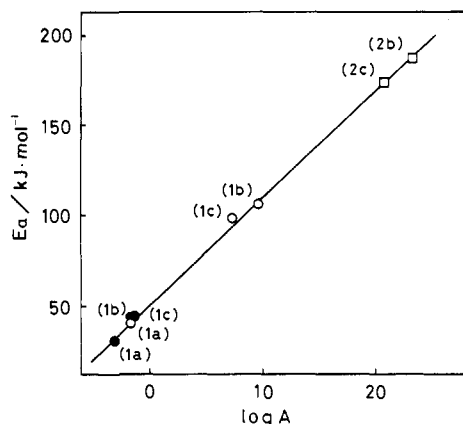


Figure 9. E_a - $\log A$ compensation relationship: open circles indicate plots for PC/EBBA/1 membranes above T_{KN} and filled circles below T_{KN} .

Table II. Rates of Ion Transport across the PC/EBBA/1a and the PC/EBBA/2b Membranes at 313 K (above T_{KN})

membrane	$10^9 P_{M^+}$ ($\text{cm}^2 \text{s}^{-1}$)			
	Na^+	K^+	Rb^+	Cs^+
PC/EBBA/1a	1.61	1.84	0	0
PC/EBBA/2b	20.3	29.4	17.3	7.89

entropy term (i.e., $\log A$: Figure 3). A similar compensation relationship has been found by Pownall et al.³⁴ for transport of pyrenylalkanes across single bilayer vesicles. Therefore, the compensation relationship may be a general feature for transport systems. It was expected that three points obtained for PC/EBBA/1 below T_{KN} might deviate from eq 1 because the transport mechanism is quite different from that above T_{KN} . In fact, these points also correlated by the line given by eq 1. Equation 2 ($r = 0.999$) computed by the least-squares procedure for eight points

$$E_a \text{ (kJ mol}^{-1}\text{)} = 5.69 \log A + 52.7 \quad (2)$$

is essentially identical with eq 1. Therefore, as long as the discussion is confined to the thermodynamic parameters, the present transport system can be expressed by a single enthalpy-entropy compensation relationship.

New Applications of Polymer/Liquid Crystal Composite Membranes. Since the K^+ transport rates in PC/EBBA/2 membranes are remarkably rapid, it is of interest to evaluate the ion selectivity of these membranes. The permeability coefficients (P_{M^+}) determined for four alkali metal cations under identical conditions are summarized in Table II and Figure 10. Examination of these transport data reveals that (i) the P_{M^+} values for the PC/EBBA/2b membrane are much greater than those for the PC/EBBA/1a membrane, (ii) the PC/EBBA/1a membrane gives almost the same transport rates for Na^+ and K^+ , whereas the PC/EBBA/2b membranes gives a maximum rate value for K^+ , and (iii) the transport of Rb^+ and Cs^+ across the PC/EBBA/1a membrane was not detected, but the efficient transport of these metal cations still takes place in the PC/EBBA/2b membrane. Finding i can be rationalized in terms of the large, positive entropy term characteristic of the fluorocarbon-containing crown ethers. The observation of ion selectivity suggests, however, that the diffusion process is not totally rate limiting but the ion extraction into the membrane phase is partially involved in the rate-limiting step. Finding (iii) that large alkali metal cations such as Rb^+ and Cs^+ can permeate through the PC/EBBA/2b membrane but not through the PC/EBBA/1a membrane could be related to the dispersion state of the ion carriers. It is known that monobenzo-15-crown-5 shows a high selectivity for Na^+ or K^+ and binds Rb^+ and Cs^+ only weakly.³⁵⁻³⁸ This is probably

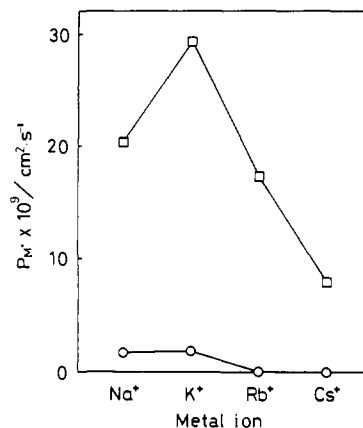


Figure 10. Ion selectivity for the transport through the PC/EBBA/1a membrane (O) and the PC/EBBA/2b membrane (□).

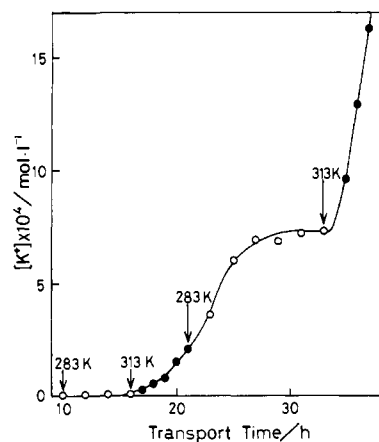


Figure 11. Temperature regulation of K^+ transport through the PC/EBBA/2b membrane.

the case for the PC/EBBA/1a membrane in which 1a is dissolved homogeneously. On the other hand, bis crown ethers and polymeric crown ethers exhibit selectivity toward large alkali metal cations because of the formation of 1:2 metal/crown sandwich complexes.³⁵⁻⁴³ Probably this is the case for the PC/EBBA/2b membrane in which 2b forms the phase-separated crown aggregates. We believe that Rb^+ and Cs^+ are extracted into the membrane phase because of the formation of such sandwich complexes. The fact that the PC/EBBA/2b membrane shows the K^+ selectivity rather than the Na^+ selectivity (finding iii) can also be rationalized in terms of the contribution of the 1:2 K^+ /crown complexes.

An all-or-nothing change in the ion permeability across the PC/EBBA/2 membranes suggests that these membranes may provide reversible thermocontrol of ion transport. Figure 11 shows the control of K^+ transport through the PC/EBBA/2b membrane by a temperature switch. In response to the temperature cycle of $283 \rightarrow 313 \rightarrow 283 \rightarrow 313$ (K), the rate of K^+ transport showed an all-or-nothing response: i.e., fast K^+ transport at 313 K (above T_{KN}) and no K^+ transport at 283 K (below T_{KN}). When the temperature was raised from 283 to 313 K for the first time, the response speed was rather slow. This is due to an induction period

(37) Gokel, G.; Korzeniowski, S. H. In *Macrocyclic Polyether Syntheses*; Springer-Verlag: Berlin, 1982.

(38) Weber, E.; Vögtle, F. In *Host Guest Complex Chemistry I*; Springer-Verlag: Berlin, 1981; p 1.

(39) Fenton, D. E. *Chem. Soc. Rev.* 1977, 6, 325.

(40) Bourgoin, M.; Wong, K. H.; Smid, J. *J. Am. Chem. Soc.* 1975, 97, 3462.

(41) Smid, J. *Makromol. Chem. Suppl.* 1981, 5, 203.

(42) Kimura, K.; Maeda, T.; Shono, T. *Makromol. Chem.* 1981, 182, 1579.

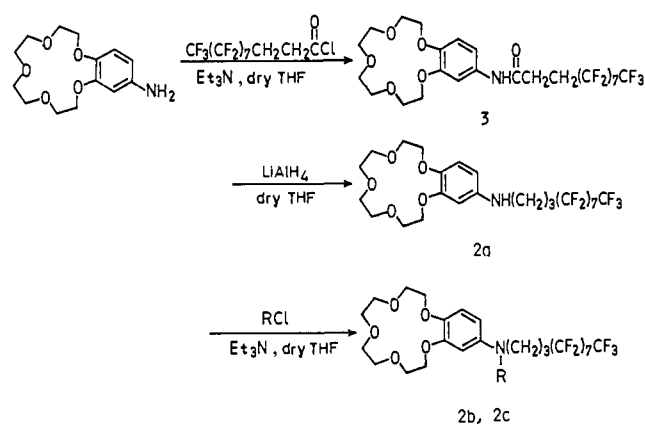
(43) (a) Wada, F.; Wada, Y.; Goto, T.; Kikukawa, K.; Matsuda, T. *Chem. Lett.* 1980, 1189. (b) Ikeda, T.; Abe, A.; Kikukawa, K.; Matsuda, T. *Chem. Lett.* 1983, 369.

(34) Pownall, H. J.; Hickson, D. L.; Smith, L. C. *J. Am. Chem. Soc.* 1983, 105, 2440.

(35) Cram, D. J.; Cram, J. M. *Acc. Chem. Res.* 1978, 11, 8.

(36) Lehn, J.-M. *Acc. Chem. Res.* 1978, 11, 49.

Scheme 1



for K^+ ions to cross the membrane. In case of the second temperature rise, K^+ transport responded very rapidly. On the other hand, the response for the temperature change from 313 to 283 K was relatively slow, taking about 6 h to suppress K^+ transport. Presumably, the transient leakage for the temperature drop stems from slow reorganization of the liquid crystal phase to the crystal phase in the polymer matrix.⁶

Conclusion. The present study demonstrates that (i) carrier-mediated ion transport is profoundly influenced by the phase separation of carriers in the membrane, (ii) the ion-transport rate through ternary composite membranes composed of the PC/EBBA/fluorocarbon-containing crown ethers can be controlled completely by a temperature switch, (iii) ion transport mediated by fluorocarbon-containing crown ethers is very fast above T_{KN} probably because of desolvation of the carrier crowns in the hydrocarbon EBBA phase, and (iv) an enthalpy-entropy compensation relationship exists in the present transport system although the transport rates are essentially governed by the entropy term. These findings have made it possible for the first time to design an ideal temperature-switched ion-transport membrane which exhibits no ion transport below T_{KN} and rapid ion transport above T_{KN} . Furthermore, findings i and iv are related to essential membrane functions and may have important implications in the functions of biomembranes. We believe that further elaboration of these findings might lead to more elegant and generalized design methods to control the membrane functions by an on-off-type temperature switch.

Experimental Section

Materials. Fluorocarbon-containing crown ethers **2a**, **2b**, and **2c** were synthesized from 4'-aminobenzo-15-crown-5 according to the reaction of Scheme 1.

4'-[N-(2''H,2'''H,3''H,3'''H-Perfluoroundecanoyl)amino]benzo-15-crown-5 (**3**). 2H,2H,3H,3H-Perfluoroundecanoyl chloride (5.24 g, 10.7 mmol) in 10 mL of anhydrous tetrahydrofuran (THF) was added dropwise to an anhydrous THF solution (120 mL) containing 4'-aminobenzo-15-crown-5 (2.83 g, 10.0 mmol) and triethylamine (2.10 g, 20.8 mmol) at room temperature under nitrogen. Progress of the reaction was followed by TLC. After 3 h, the precipitate was filtered, and the filtrate was concentrated to dryness in vacuo. The residue was dissolved in chloroform and washed with dilute aqueous HCl (pH 3). The chloroform solution was evaporated to dryness and the residue was recrystallized from ethanol in the presence of activated charcoal: single spot on TLC, mp 129–131 °C, yield 71%. Fluorocarbon-containing compounds cannot be subjected to elemental analysis because they may damage the glassware apparatus upon combustion. Thus, the purity was confirmed by TLC and ¹H NMR: IR (KBr) $\nu_{C=O}$ 1665, ν_{COC} 1145 cm^{-1} ; ¹H NMR (CDCl₃) δ 2.54 (4 H, CF₂CH₂CH₂), 3.71, 3.86, 4.04 (8 H, 4 H, 4 H, crown protons), 6.70, 6.81, 7.24 (1 H, 1 H, 1 H, aromatic protons), 7.55 (1 H, NH).

4'-[N-(1''H,1'''H,2''H,2'''H,3''H,3'''H-Perfluoroundecyl)amino]benzo-15-crown-5 (**2a**). **3** (3.00 g, 4.00 mmol) in 220 mL of anhydrous THF was heated with LiAlH₄ (1.0 g, 26 mmol) under reflux for 4 h. After the mixture cooled, the remaining LiAlH₄ was decomposed by addition of water, and the precipitate was removed by filtration. The filtrate was concentrated to dryness in vacuo, and the residue was recrystallized from diethyl ether in the presence of activated charcoal: one

spot on TLC, mp 82–84 °C, yield 41%; IR (KBr) $\nu_{C=O}$ 1130 cm^{-1} (no $\nu_{C=O}$); ¹H NMR (CDCl₃) δ 1.94 (2 H, 2''-CH₂), 2.12 (2 H, 3''-CH₂), 3.14 (2 H, 1''-CH₂), 3.72, 3.88, 4.05 (8 H, 4 H, 4 H, crown protons), 6.19, 6.73 (2 H, 1 H, aromatic protons), 6.80 (1 H, NH).

4'-[N-Butyryl-N-(1''H,1'''H,2''H,2'''H,3''H,3'''H-perfluoroundecyl)amino]benzo-15-crown-5 (**2b**). Butyryl chloride (0.13 g, 1.2 mmol) in 10 mL of anhydrous THF was added dropwise to an anhydrous THF solution (20 mL) of **2a** (0.81 g, 1.0 mmol) and triethylamine (0.21 g, 2.1 mmol) at room temperature under nitrogen. After 3 h, the mixture was filtered, and the filtrate was evaporated to dryness in vacuo. The residue was dissolved in benzene, and the solution was washed with an acidic (pH 3) aqueous solution, a 0.05 M LiOH solution, and water. The benzene solution was evaporated to dryness in vacuo, and the residue was separated by preparative TLC (silica gel, chloroform:methanol = 15:1 v/v): single spot on TLC, mp 56–58 °C, yield 50%; IR (KBr) $\nu_{C=O}$ 1650, ν_{COC} 1135 cm^{-1} ; ¹H NMR (CDCl₃) δ 0.80, 1.24, 1.48 (3 H, 2 H, 2 H, butyryl), 1.96 (2 H, 2''-CH₂), 2.04 (2 H, 3''-CH₂), 3.70 (2 H, 1''-CH₂), 3.80, 4.00, 4.20 (8 H, 4 H, 4 H, crown protons), 6.76, 6.82, 6.96 (1 H, 1 H, 1 H, aromatic protons).

4'-[N-Dodecanoyl-N-(1''H,1'''H,2''H,2'''H,3''H,3'''H-perfluoroundecyl)amino]benzo-15-crown-5 (**2c**). Compound **2c** was prepared from **2a** (0.37 g, 0.50 mmol) and dodecanoyl chloride (0.15 g, 0.69 mmol) in a manner similar to the synthesis of **2b**. The product was isolated by a preparative TLC (silica gel, chloroform:methanol = 30:1 v/v): one spot on TLC, oil, yield 69%; IR (neat) $\nu_{C=O}$ 1650, ν_{COC} 1120 cm^{-1} ; ¹H NMR (CDCl₃) δ 0.84, 1.20, 1.50 (3 H, 18 H, 2 H, dodecyl), 1.90 (2 H, 2''-CH₂), 2.01 (2 H, 3''-CH₂), 3.63 (2 H, 1''-CH₂), 3.73, 3.92, 4.09 (8 H, 4 H, 4 H, crown protons), 6.57, 6.66, 6.84 (1 H, 1 H, 1 H, aromatic protons).

4'-[N-Dodecanoylamino]benzo-15-crown-5. This compound was prepared from 4'-aminobenzo-15-crown-5 (1.42 g, 5.0 mmol) and dodecanoyl chloride (1.32 g, 6.00 mmol) in a manner similar to the synthesis of **3**. The product was recrystallized from ethanol in the presence of activated charcoal: single spot on TLC, mp 108–110 °C, yield 67%; IR (KBr) $\nu_{C=O}$ 1655, ν_{COC} 1140 cm^{-1} .

4'-[N-Dodecylamino]benzo-15-crown-5. This compound was prepared by the reduction of 4'-[N-(dodecanoyl)amino]benzo-15-crown-5 (1.40 g, 3.10 mmol) by LiAlH₄ (0.70 g, 180 mmol). The product was recrystallized from diethyl ether in the presence of activated charcoal: mp 57–59 °C, yield 56%; IR (KBr) ν_{COC} 1130 cm^{-1} (no $\nu_{C=O}$). Anal. (C₂₆H₄₅NO₃) C, H, N (this description indicates that satisfactory analytical data ($\pm 0.4\%$ for C, H, N, etc.) were reported).

Hydrocarbon-containing crown ethers (**1a**, **1b**, and **1c**) were synthesized from 4'-[N-(dodecyl)amino]benzo-15-crown-5 and the corresponding acid chlorides in a manner similar to the synthesis of **2**.

4'-[N-Butyryl-N-dodecylamino]benzo-15-crown-5 (**1a**). Oil, single spot on TLC, yield 75%; IR (neat) $\nu_{C=O}$ 1650, ν_{COC} 1130 cm^{-1} ; ¹H NMR (CDCl₃) δ 0.86, 1.26, 1.54, 2.04, 3.60 (6 H, 20 H, 2 H, 2 H, 2 H, butyryl and dodecyl), 3.85, 4.00, 4.20 (8 H, 4 H, 4 H, crown protons), 6.74, 6.82, 6.92 (1 H, 1 H, 1 H, aromatic protons). Anal. (C₃₀H₅₁NO₆) C, H, N.

4'-[N-(*p*-Toluenesulfonyl)-N-dodecylamino]benzo-15-crown-5 (**1b**): mp 71–73 °C, yield 37%; IR (KBr) ν_{SO_2} 1155, 1340, ν_{COC} 1140 cm^{-1} ; ¹H NMR (CDCl₃) δ 0.86, 1.16, 3.36 (3 H, 20 H, 2 H, dodecyl), 2.32, 7.04, 7.32 (3 H, 2 H, 2 H, *p*-toluenesulfonyl), 3.64, 3.80, 4.00 (8 H, 4 H, 4 H, crown protons), 6.40, 6.52, 6.64 (1 H, 1 H, 1 H, aromatic protons). Anal. (C₃₃H₅₁NO₇S) C, H, N.

4'-[N-(*p*-Toluoxy)-N-dodecylamino]benzo-15-crown-5 (**1c**): oil, single spot on TLC, yield 60%; IR (neat) $\nu_{C=C}$ 1640, ν_{COC} 1140 cm^{-1} ; ¹H NMR (CDCl₃) δ 0.80, 1.16, 3.60 (3 H, 20 H, 2 H, dodecyl), 2.16, 6.84, 7.07 (3 H, 2 H, 2 H, *p*-toluoxy), 3.63, 3.78, 3.98 (8 H, 4 H, 4 H, crown protons), 6.42, 6.50, 6.56 (1 H, 1 H, 1 H, aromatic protons). Anal. (C₃₄H₅₁NO₆) C, H, N.

Preparation and Characterization of Composite Membranes. The composite membranes were prepared by casting a 6 wt % (total) 1,2-dichloroethane solution of PC (supplied from Idemitsu Kosan Co.), EBBA, and a crown ether on a glass plate at room temperature: PC:EBBA = 40:60 wt/wt and crown ether:EBBA = 3:70 mol/mol (i.e., 9.3×10^{-5} mol/g (PC + EBBA)) unless otherwise stated. PC was selected as the matrix polymer for the composite membranes because it has no thermal transition in the temperature range studied here.⁷ After 1 day, the membranes were dried at 0.1 mmHg for 4 h and then kept under reduced pressure for 3 days. The thickness of the membranes thus obtained was 70 ± 3 m. In the transport experiments, the membrane surface in contact with the glass plate was always directed toward the IN aqueous phase.

The dispersion state of the crown ethers in these composite membranes are investigated by DSC (Daini Seikosha SSC-560).

Ion Transport. Ion transport across the composite membranes was carried out in a U-tube immersed in a thermostated water bath. The membrane area was 3.46 cm², and the IN and OUT aqueous phases (30

mL each) were stirred at a constant speed (ca. 250 rpm). Further details of the transport method were described previously.⁶ The rates of ion transport were estimated by measuring the concentration of alkali metal cations transported to the OUT aqueous phase by atomic absorption spectroscopy (Shimadzu AA-640). One transport experiment was continued at least for 20 h, and the ion flux (J , mol s⁻¹ cm⁻²) was determined from the linear slope of the $[M^+]$ vs. time plot. The permeability coefficients (P_{M^+} , s⁻¹ cm²) were calculated from eq 3, where l is the mem-

brane thickness and C_{IN} and C_{OUT} are the metal concentrations in the IN and the OUT aqueous phase, respectively.

$$P_{M^+} = Jl / (C_{IN} - C_{OUT}) \quad (3)$$

Acknowledgment. This research was partly supported by the Grant-in-Aid on Special Project Research from the Ministry of Education, Science and Culture.

[1-¹³C]Aldono-1,4-lactones: Conformational Studies Based on ¹H-¹H, ¹³C-¹H, and ¹³C-¹³C Spin Couplings and ab Initio Molecular Orbital Calculations

Timothy Angelotti, Michael Krisko, Thomas O'Connor, and Anthony S. Serianni*

Contribution from the Department of Chemistry, University of Notre Dame, Notre Dame, Indiana 46556. Received July 3, 1986

Abstract: Several aldono-1,4-lactones have been synthesized with [¹³C] enrichment (99 atom %) at the carbonyl carbon. ¹H (300 and 600 MHz) and ¹³C (75 MHz) NMR spectra in ²H₂O have been assigned, the latter with the aid of 2D ¹³C-¹H chemical shift correlation spectroscopy. ¹H-¹H, ¹³C-¹H, and ¹³C-¹³C couplings have been used to evaluate lactone ring conformations. In general, aldono-1,4-lactones in aqueous solution prefer conformations in which O2 is oriented quasi-equatorial. On the basis of ab initio STO-3G MO calculations of two representative lactones, it appears that this preference is not due to stabilization conferred by intramolecular hydrogen bonding, as generally believed, but to stereoelectronic factors found in α -hydroxy- γ -lactones. Theoretical calculations have also revealed a notable effect of lone-pair oxygen orbitals on C-H bond lengths, namely, that C-H bonds are longest when antiperiplanar to a lone-pair orbital. This dependence may be responsible, in part, for the observed ¹H chemical shift patterns for these molecules. A model has been proposed to rationalize the dependence of dual-pathway ¹³C-¹³C couplings on lactone ring configuration.

The conformational characteristics of five-membered rings have been the subject of scientific scrutiny for decades.¹ This interest has been stimulated in recent years because of the potential role that furanose ring conformation and dynamics play in the structure and function of nucleic acids in biological systems.² The simplest saturated five-membered ring, cyclopentane, exists in puckered (envelope, twist) conformations in solution^{1d,e} in which the destabilizing effects of eclipsed C-H bonds are minimized. As either endocyclic or exocyclic heteroatoms are substituted/append to the ring, additional molecular forces compete to determine preferred geometry.³ Twenty puckered conformers can be assumed by dissymmetric furanose rings (10 envelope, 10 twist), and their spontaneous interconversion occurs by pseudorotation.^{1a,4} In general, these conformers have similar energies. Conformational averaging, therefore, complicates the interpretation of the physical constants (e.g., NMR parameters)⁵ of these structures.

We have shown that conformational analysis of furanose rings by NMR spectroscopy is notably improved by measuring ¹³C-¹H and ¹³C-¹³C in addition to ¹H-¹H spin couplings in these rings.³ Perlin and co-workers⁶ have made similar arguments, namely, that

Table I. Preparation and Purification of D-[1-¹³C]Aldonates

compound	method ^a	chromatography ^b
erythro 1	A	0.5 M
threo 5	A	0.5 M
arabino 6, ribo 2	B	0.35 M (2 L), then 0.5 M (3 L): ribo
lyxo 12, xylo 9	B	0.4 M (4 L): xylo
allo 3, altro 7	B	0.4 M (4 L): allo
galacto 8, talo 4	B	0.1-0.4 M LG ^c (4 L), followed by 0.4 M (2 L): talo
gluco 10, manno 13	B	0.7 M (3 L): gluco

^aMethod A: hypiodite oxidation of the corresponding D-[1-¹³C]-aldose. Method B: cyanohydrin synthesis. ^bDowex 1 \times 8 (200-400 mesh) in the acetate form; column size = 2.5 \times 60 cm. Acetic acid was employed as the eluent using the concentrations and volumes indicated. Columns were eluted at a flow rate of \sim 1 mL/min (15-mL fractions), and fractions were assayed for aldinate with chromatographic acid.¹³ The epimer that elutes first is identified. ^cLG = linear gradient.

"redundant" coupling measurements often improve the discrimination between conformers.

Replacement of a furanose ring sp³ carbon by an sp² carbon (e.g., conversion to an aldono-1,4-lactone) causes considerable changes in ring conformation and dynamics. The planarity (or near-planarity) of the OC(O)C fragment restricts 1,4-lactone rings to two relatively small segments of the pseudorotational itinerary.⁴ Because 1,4-lactone rings are important components of many natural products (e.g., antibiotics), we have examined the structural properties of several [1-¹³C]aldono-1,4-lactones in aqueous (²H₂O) solution by ¹H and ¹³C NMR spectroscopy. ¹H and ¹³C chemical shifts have been assigned, and ¹H-¹H, ¹³C-¹H, and ¹³C-¹³C coupling constants have been measured and related

(1) (a) Kilpatrick, J.; Pitzer, K.; Spitzer, K. *J. Am. Chem. Soc.* **1947**, *69*, 2485. (b) Altona, C.; Sundaralingam, M. *Ibid.* **1972**, *94*, 8205. (c) Gerlt, J. A.; Youngblood, A. V. *Ibid.* **1980**, *102*, 7433. (d) Poupko, R.; Luz, Z.; Zimmermann, H. *Ibid.* **1982**, *104*, 5307. (e) Cremer, D.; Pople, J. A. *Ibid.* **1975**, *97*, 1358.

(2) (a) de Leeuw, H. P. M.; Haasnoot, C. A. G.; Altona, C. *Isr. J. Chem.* **1980**, *20*, 108. (b) Levitt, M.; Warshel, A. *J. Am. Chem. Soc.* **1978**, *100*, 2607. (c) Olson, W. K.; Sussman, J. L. *Ibid.* **1982**, *104*, 270. (d) Olson, W. K. *Ibid.* **1982**, *104*, 278. (e) Westhof, E.; Sundaralingam, M. *Ibid.* **1983**, *105*, 970.

(3) Serianni, A. S.; Barker, R. *J. Org. Chem.* **1984**, *49*, 3292.

(4) Altona, C.; Sundaralingam, M. *J. Am. Chem. Soc.* **1972**, *94*, 8205.

(5) Jardetsky, O. *Biochem. Biophys. Acta* **1980**, *621*, 227.

(6) Cyr, N.; Perlin, A. S. *Can. J. Chem.* **1979**, *57*, 2504.